Nano Energy 134 (2025) 110526

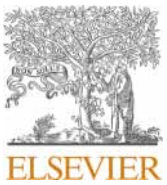

Contents lists available at ScienceDirect

Nano Energy

journal homepage: www.elsevier.com/locate/nanoen

Contact-electro-chemistry induced by flow electrification in dielectric tubes☆

Chong Xu [a,b], Shaoxin Li [a,b], Yuyang Zhang [c], Ziming Wang [a], Zhong Lin Wang [a,d,*], Di Wei [a,e,*]

[a] Beijing Institute of Nanoenergy and Nanosystems, Chinese Academy of Sciences, Beijing 101400, PR China
[b] School of Nanoscience and Engineering, University of Chinese Academy of Sciences, Beijing 100049, PR China
[c] Department of Material Science and Engineering, The University of Manchester, M13 9PL, UK
[d] Beijing Key Laboratory of Micro-Nano Energy and Sensor, Center for High-Entropy Energy and Systems, Beijing Institute of Nanoenergy and Nanosystems, Chinese Academy of Sciences, Beijing 101400, PR China
[e] Centre for Photonic Devices and Sensors, University of Cambridge, 9 JJ Thomson Avenue, Cambridge CB3 0FA, UK

ARTICLE INFO

Keywords:
Contact-electro-chemistry
Flow electrification
Triboelectric charge
Reactive oxygen species
Physical parameters of tubes

ABSTRACT

Although liquid-solid contact electrification (CE) is a long-established natural phenomenon, few systematic studies have explored the triboelectric charge-induced chemical reactions it initiates, particularly the reactions caused by flow electrification (FE) within dielectric tubes over long distances. Here, a tunable and easily recyclable contact-electro-chemistry (CE-Chemistry) method is presented, employing triboelectric charge from FE to directly monitor general chemical reactions, such as $[Fe(CN)_6]^{4-}$ oxidation, $[AuCl_4]^-$ reduction, and luminol luminescence etc. The chemical reaction rate could be regulated by physical parameters of dielectric tubes, including input flow velocity, tube inner diameter, length, and series-parallel configurations etc. Additionally, cascade reaction could be designed by simulating the Flow Injection Analysis (FIA) facilities, originally used in analytical chemistry. The CE-Chemistry induced by FE in dielectric tubes holds potential for real-time catalysis of organic waste and reduction of precious metals in wastewater tubes, prompting a reconsideration of the effectiveness of some traditional analytical chemistry methodologies utilizing flow-based systems such as high-performance liquid chromatography (HPLC).

1. Introduction

In nature, the continuous interaction between liquid and solid often reveals significant physicochemical phenomena. For instance, flowing water resists stagnation, while hydraulic forces exert mechanical pressure on rock surfaces, leading to erosion and the displacement of particles, which profoundly alters the chemical composition and structure of the rocks [1,2]. The study of liquid-solid interfaces is pivotal for advancing fundamental understanding in materials science, catalysis, and energy storage etc. [3–6], as these interfaces play a crucial role in governing interfacial reactions and charge transfer processes. Insights from this research can guide the development of more efficient systems, thereby improving performance across various applications. Most chemical reactions are driven by charge transfer processes occurring at liquid-solid interfaces that inherently involve contact electrification (CE) phenomenon [7,8]. Thus, understanding chemical reactions at liquid-solid interfaces from the perspective of liquid-solid CE is fundamentally significant, as it elucidates the mechanisms governing interfacial processes that impact various reactions. Additionally, the CE effect inherently arises at liquid-solid interfaces during relative motion. For instance, as a liquid droplet flows across a solid surface, it imparts charge to the surface of liquid and solid respectively. This phenomenon enables not only the regulation of surface charge through droplet manipulation, but also influencing chemical reactions as well. Zhang et al. proposed that the positively charged luminol droplet generated by sliding on the Polytetrafluoroethylene (PTFE) dielectric polymer surface will increase the reaction reactivity and enhance the chemical luminescence intensity, although the reaction's visibility is somewhat

☆ Prof Zhong Lin Wang, an author on this paper, is the Editor-in-Chief of Nano Energy, but he had no involvement in the peer review process used to assess this work submitted to Nano Energy. This paper was assessed, and the corresponding peer review managed by Professor Chenguo Hu, also an Associate Editor in Nano Energy.

* Corresponding authors at: Beijing Institute of Nanoenergy and Nanosystems, Chinese Academy of Sciences, Beijing 101400, PR China.
E-mail addresses: zhong.wang@mse.gatech.edu (Z.L. Wang), dw344@cam.ac.uk (D. Wei).

https://doi.org/10.1016/j.nanoen.2024.110526
Received 22 October 2024; Received in revised form 13 November 2024; Accepted 27 November 2024
Available online 29 November 2024

limited by the small droplet volume [9].

Furthermore, chemical reactions induced by CE at liquid-solid interfaces have garnered significant interest in green chemistry, where electron transfer, a fundamental mechanism of CE, catalyzes radical formation and initiates a series of reactions under strong mechanical stimuli, such as ultrasonication and ball milling [10,11]. This paradigm-shift technology, termed contact-electro-catalysis (CEC), opens up exciting possibilities for the development of innovative catalysts and chemical processes. For instance, the degradation of organic pollutant, the generation of hydrogen peroxide (H_2O_2) [12,13], the recycling of cathode materials in spent lithium-ion batteries [14], the reduction of precious metals from aqueous solutions [15], and other applications envisioned to be applied in cancer therapy etc. [16] CEC enables traditionally inert polymers to act as catalysts. Additionally, our prior research has extended this methodology to various applications, including polyaniline synthesis, luminol luminescent reactions, and redox processes. A unified framework integrating work functions, electronegativity within the triboelectric series, and standard electrode potentials has also been developed, leading to the introduction of the concept of contact-electro-chemistry (CE-Chemistry) based on electron transfer capabilities [17,18]. In CE-Chemistry, traditionally inert polymers such as Fluorinated Ethylene Propylene (FEP) and PTFE are commonly employed as ideal dielectrics to CE for generating radicals and facilitating reactions. Strong mechanical conditions, including ultrasonication or ball milling [10,11], are generally employed to enhance liquid-solid CE performance, thereby intensifying observable CE-chemical reaction. However, CE-chemical reactions under mild mechanical stimulation remain underexplored, despite the ubiquity of CE at liquid-solid interface and its growing impact on the field of organic synthesis and analytical chemistry.

Here, we confirmed the existence of CE-Chemistry under mild mechanical stimulation via flow electrification (FE) and further introduced a tunable and easily recyclable CE-Chemistry method. This approach leverages triboelectric charge generated from FE between flowing liquids and solid dielectric tubes. FEP tubes served as both CE dielectrics and direct reaction vessel, enabling flexible regulation of CE-Chemistry by physical parameters, including input flow velocity, tube inner diameter, length, and series-parallel configurations etc. The optimized reaction parameters are an input flow velocity of 0.05 mL/s and a 5 m-parallel configuration. The oxidation of potassium ferrocyanide ($K_4[Fe(CN)_6]$) and luminescence of luminol were directly observed. Furthermore, a reusable method facilitated the degradation of the organic dye

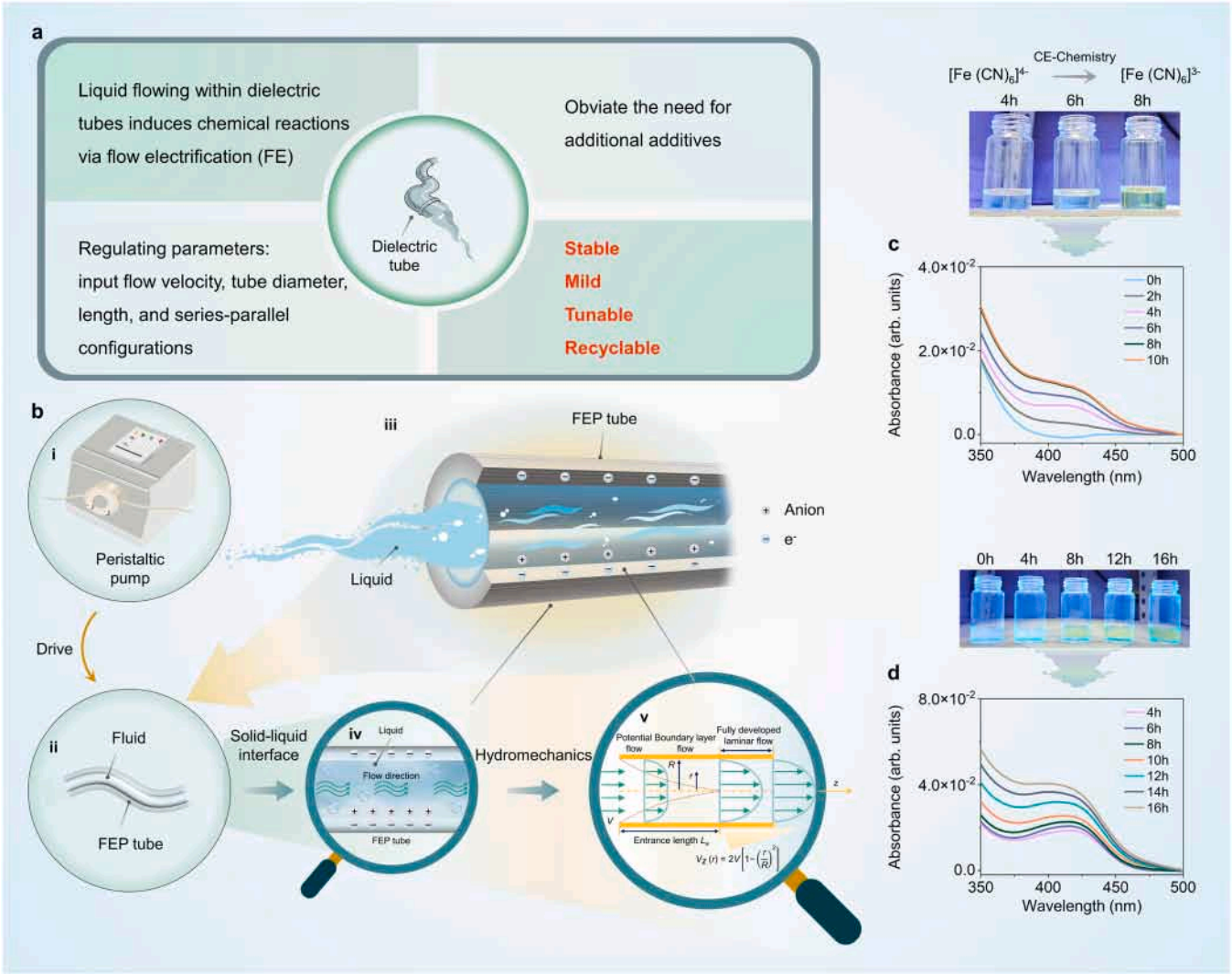

Fig. 1. CE-Chemistry for $K_4[Fe(CN)_6]$ solution and FEP tubes. (a) USP of CE-Chemistry induced by flow electrification (FE) in dielectric tubes. (b) The overall skeleton diagram of the CE-Chemistry between fluid and dielectric tubes. (i) The source of mechanical energy. (ii) Fluid in FEP tube. (iii) The local magnification of the fluid in FEP tube. (iv) Charge transfer induced by CE between the solid-liquid interface. (v) The theory of hydromechanics between fluid and tube. (c) Oxidation of $[Fe(CN)_6]^{4-}$ from 0 hour to 10 hour and optical photographs of solution color change. (d) Oxidation of $[Fe(CN)_6]^{4-}$ from 10 hour to 16 hour by cleaning the initial surface charge with alcohol and optical photographs of solution color change.

methyl orange (MO) and the reduction of precious metal (Au^0) from ($[AuCl_4]^-$) under mild and tunable conditions. This demonstrates its potential for real-time catalysis of organic waste and the recycling of heavy metals in wastewater systems. It should be also noted that the oxidation of $K_4[Fe(CN)_6]$ and the luminescence of luminol exemplify a cascade reaction that can be effectively realized through simulation of Flow Injection Analysis (FIA) systems. This finding suggests a need for critical reevaluation of all analytical methodologies utilizing flow-based systems, including high-performance liquid chromatography (HPLC), in light of the chemical reactions potentially induced by the triboelectric charges generated from FE.

2. Results and discussion

2.1. CE-Chemistry for $K_4[Fe(CN)_6]$ solution and FEP tubes

Compared to the pronounced physical forces generated by methods such as ultrasonication or ball milling commonly used in CE-Chemistry, the reactions induced by FE in flowing liquids within dielectric tubes are often overlooked. However, once established, the tunability of this approach could prove substantial, offering significant advantages in terms of stability, mildness, ease of regulation and recyclability (Fig. 1a). Crucially, the dielectric tubes serve not only as liquid carriers but also as catalysts, initiating reactions via FE. Unlike prior CE-Chemistry approaches that necessitate the incorporation of solid dielectric powders or films into contained solutions, this method obviates the need for such additives. Furthermore, it could offer a direct mechanism for regulating CE efficiency based on hydromechanics. Thus, the FE method in CE-Chemistry potentially offers a means to affect chemical reactions through the regulation of physical parameters such as input flow velocity, tube inner diameter, length, and series-parallel configurations. Fig. 1b illustrated the overall schematic of the CE-Chemistry via the FE method, comprising a peristaltic pump (Fig. 1b (i)) and dielectric tubes (Fig. 1b (ii)). The peristaltic pump ensured stable fluid flow through FEP tubes, commonly used in chemical analysis and flow injection systems. A detailed view of the fluid in the FEP tubes was presented in Fig. 1b (iii), highlighting that electron transfer primarily occurred at the liquid-solid interface (Fig. 1b (iv)). Moreover, the CE performance is influenced by mechanical stimulation, emphasizing the consideration of hydrodynamic effects on CE in this study (Fig. 1b (v)). The explain of potential flow, boundary layer flow, fully developed laminar flow and the equation are shown in Note 1 [19]. Generally, the flow velocity at the center of the tube differs from that at the wall due to frictional forces. Additionally, flow velocity is influenced by various physical parameters, such as the length and inner diameter of the tube, which can regulate the interfacial charge exchange performance between solid and liquid phases, subsequently impacting the charge exchange chemical reaction. The photograph of Fig. 1c showed the color of 0.1 mM $K_4[Fe(CN)_6]$ solution changed from transparent to light yellow when it flowed in the FEP tubes after different time interval. As illustrated in Fig. S1, no UV-Vis absorption peak at 420 nm was detected in the 0.1 mM standard $K_4[Fe(CN)_6]$ solution, whereas a pronounced peak was observed in the 0.1 mM standard $K_3[Fe(CN)_6]$ solution. According to experimental observations, the UV-Vis absorption peak at 420 nm intensified with the increasing flow time of the $K_4[Fe(CN)_6]$ solution in the tubes, indicating the generation of $K_3[Fe(CN)_6]$ due to the oxidation of $K_4[Fe(CN)_6]$. Moreover, the elevated UV-Vis peak at 420 nm for the flowing $K_4[Fe(CN)_6]$ solution in FEP tubes, compared to the stationary solution after 3 hours, underscores the critical role of FE in the oxidation reaction (Fig. S2). In general, FEP extracts electrons from water molecules, leading to the generation of oxidized free radicals that enhance the oxidation reaction. Notably, the electron transfer efficiency in CE is influenced by the ionic concentration of the solution, which in turn affects the formation of the electrical double layer (EDL). This theory supported the results in Fig. S3, where the UV-Vis peak at 420 nm decreased as the increasing electrolyte concentration of potassium chloride (KCl). Specifically, the oxidation reaction induced by FE is inhibited in high ionic concentration environments due to excess ions adsorption onto the negatively charged FEP tubes, forming an EDL that reduces electron transfer and diminishes reaction efficiency. Consequently, the oxidation efficiency of the $K_4[Fe(CN)_6]$ solution diminishes over time, as indicated by the UV-Vis spectra at 8 and 10 hours in Fig. 1c. This decline is likely due to the formation of an electrical double layer (EDL) resulting from the accumulation of positive ions on the negatively charged FEP tubes after they capture electrons from water molecules. Notably, as illustrated in Fig. 1d, reaction efficiency was restored after 16 hours by cleaning the inner surface of the FEP tubes with alcohol and subsequent drying, as alcohol effectively removes the initial surface charge of the FEP [20]. This demonstrates the recyclability and reusability of the FE method in CE-Chemistry.

2.2. Impact of flow tube physical parameters on chemical reactions

According to the "electron-cloud-potential-well" model in CE mechanism, electron transfer occurs at the interface when the electron clouds of two atoms overlap with the reduced potential barrier [21]. As illustrated in Fig. 2a (i) and 2a (ii), electrons transfer from the high energy level of water to FEP during the initial charge exchange due to the overlap of electron clouds when water molecules collide with FEP. As the fluid flows through the tube, similar electron exchanges occur during FE. The boundary layer between the solid and fluid phases suggests this overlap of electron clouds, as evidenced by the COMSOL simulation of flow within the FEP tubes. Fig. 2b illustrated the COMSOL simulation of 3D flow rate of the fluid in FEP tubes under a steady state, with the input flow velocity 0.15 m/s. The simulation used a low Reynold number k-ε model, which considered the need for high velocity resolution around the tube wall. Compare to other models such as Large Eddy Simulation (LES) and Direct Numerical Simulation (DNS) model, the low Reynold number k-ε model can describe the boundary layer more accurately, which is more suitable for our research and has lower computational cost. It can be seen that the flow rate of liquid at the boundary layer is lower than that at the inner position, indicating the presence of a resistance force at the boundary layer between liquid and FEP tubes. Therefore, by integrating the electron transfer mechanism of CE with a hydromechanical model, electron transfer might occur at the boundary layer due to flow resistance interactions between the liquid and the FEP tubes, thereby initiating various chemical reactions.

Consequently, the influence of physical parameters of the tubes on CE-Chemistry via FE was systematically investigated, including input flow velocity, inner diameter, and length of the FEP tubes, all under a liquid volume of 2 mL. In this work, the optimized oxidation of $K_4[Fe(CN)_6]$ was achieved at an input flow velocity of 0.05 mL/s, as shown in Fig. 2c and Fig. S4. Various input flow velocities were generated by adjusting the preset rotational speeds of the peristaltic pumps (Table S1). Additionally, the inner flow velocities within the tube at different preset input velocities were simulated using COMSOL (Fig. S5). This simulation assessed the flow rate from the center of the tube (0 mm) to the inner wall (0.25 mm, corresponding to the tube's radius). The results indicate that the boundary layer between the tube wall and the liquid varies with input flow velocities (0.01 mL/s, 0.03 mL/s, 0.05 mL/s, 0.07 mL/s), potentially influencing the frictional resistance between the fluid and the solid surface. Additionally, the larger size (inner diameter) of the tube, the lower the flow rate will be, resulting in the better reaction in the 1.6 mm-diameter tube compared to 0.5 mm and 1.0 mm diameter. (Fig. 2d and Fig. S6). As illustrated in Fig. 2e, longer lengths of the FEP tube exhibited improved reaction efficiency, likely attributable to increased opportunities for CE. Thus, CE-Chemistry via FE can be potentially regulated by various physical parameters, including input flow velocity, tube inner diameter, and length, highlighting its controllability.

Furthermore, the design of FEP tubes using FE is illustrated through various series-parallel configurations in Fig. 2f, including 5 m-series, (2

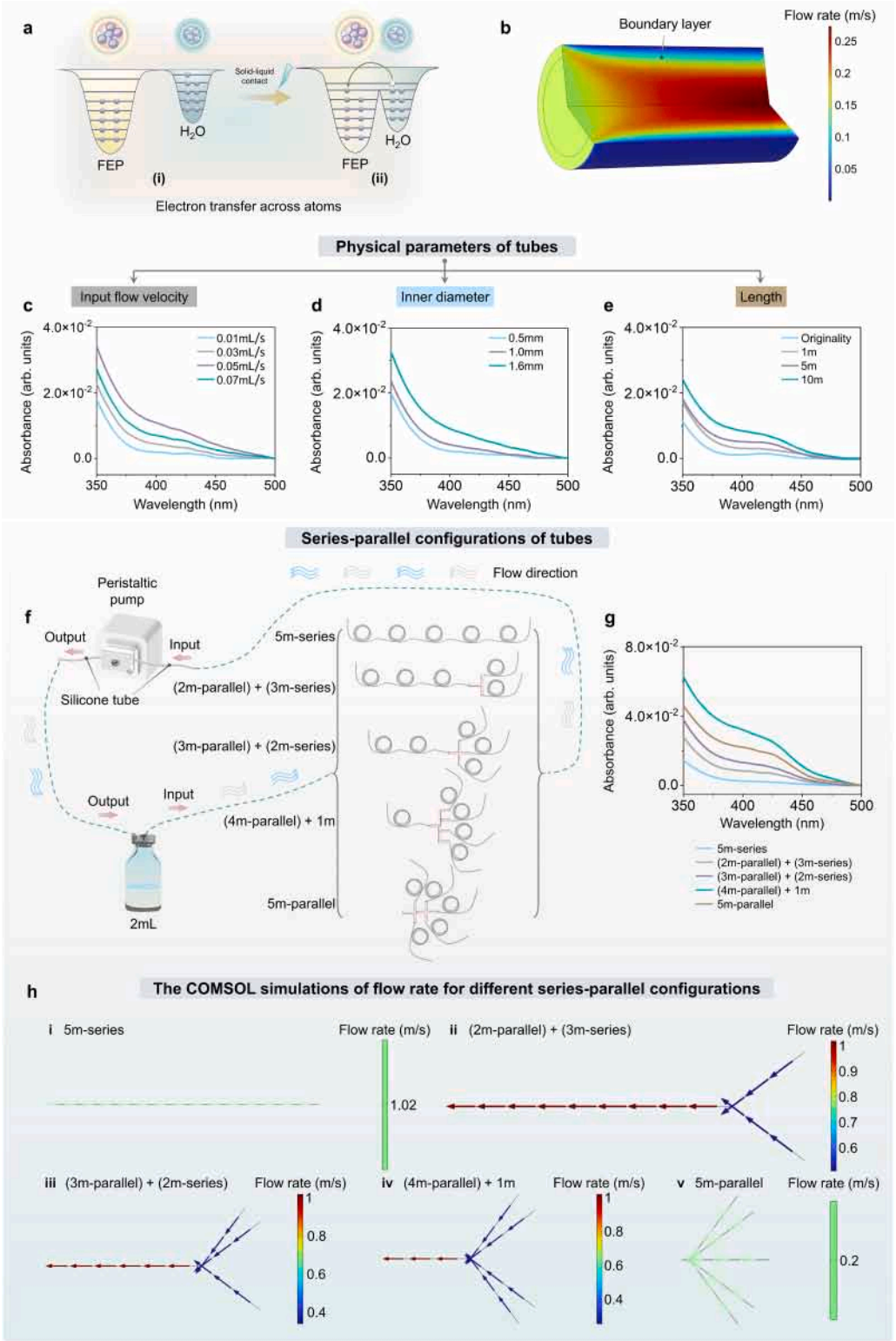

Fig. 2. The effect of modulating the physical parameters of the flow tubes on the chemical reaction. (a) Schematic of the electron cloud and potential energy profile (2D) of two atoms belonging to two materials A and B, respectively, when they are: (i) before contact, (ii) in contact. (b) 3D flow rate simulation of the fluid in the FEP tube. The influence of (c) input flow velocity, (d) inner diameter and (e) length of the FEP tubes on CE-Chemistry. (f) The five different configurations of connecting FEP tubes in series and parallel. (g) The influence of five series-parallel configurations on the results of oxidation of $[Fe(CN)_6]^{4-}$. (h) The flow rate of different series-parallel configurations in the tubes simulated by COMSOL. i-v are 5m-series, (2m-parallel)-(3m- series), (3m-parallel)-(2m- series), (4m-parallel)-1m, and 5m-parallel respectively.

m-parallel) + (3 m-series), (3 m-parallel) + (2 m-series), (4 m-parallel) + 1 m, 5 m-parallel. With the same total length of FEP tubes and rotational speed of the peristaltic pumps, the reaction performance of parallel configurations surpasses that of series configurations. Moreover, increasing the number of branches in parallel configurations (5 m-parallel) further enhances reaction performance (Fig. 2g and Fig. S7). The design of parallel tubes minimizes flow rate in each tube under the same peristaltic pump power, as the fluid can traverse multiple pathways. Moreover, the flow rates of each tube for different configurations were simulated by COMSOL in Fig. 2h. The tubes are modeled as cylindrical structures, and roughness is calculated using the Churchill model, which effectively simulates a wide range of scenarios, including varying Reynolds numbers. The configurations i-v represent 5 m-series, (2 m-parallel) + (3 m-series), (3 m-parallel) + (2 m-series), (4 m-parallel) + 1 m, and 5 m-parallel, respectively. The flow rate in each parallel tube is slower than that in the series tubes, resulting in more effective contact with the tube walls, which enhances the CE effect. Consequently, the 5 m-parallel configuration demonstrates superior CE-chemical reaction performance compared to the other configurations.

2.3. Mechanism of CE-chemistry induced by FE

In order to further understand the underlying mechanism of CE-Chemistry induced by triboelectric charge of FE, the production of

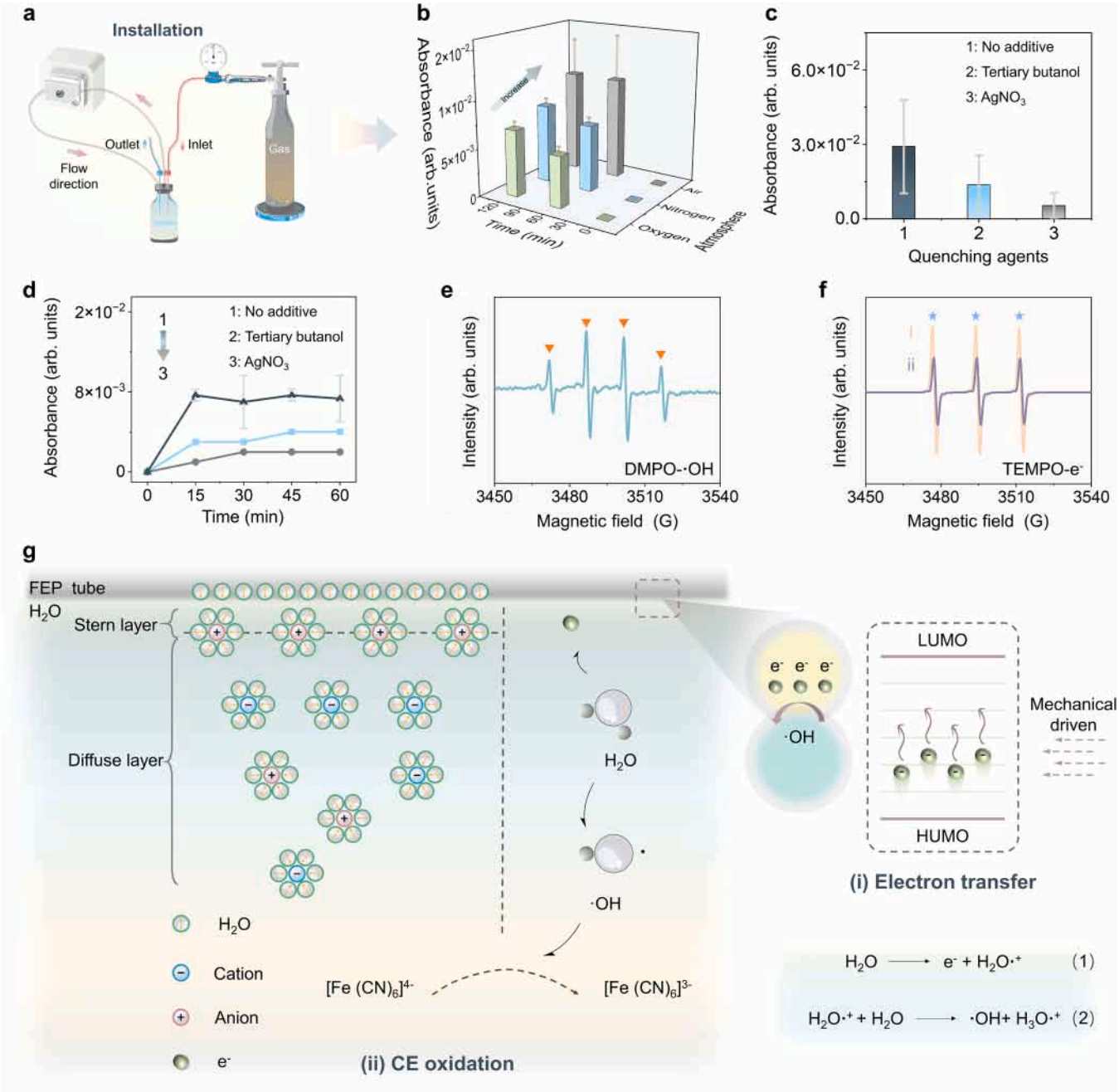

Fig. 3. Mechanism of CE-Chemistry initiated by triboelectric charge of flow electrification. (a) The installation of ventilation. (b) The effect of constantly bubbling air, N_2, or O_2 on the reaction rate. (c) The evolution of $[Fe(CN)_6]^{3-}$ concentration in presence of quenchers. Ter-butanol and $AgNO_3$ are regarded as hydroxide radical and electron quenchers, respectively. (d) The evolution of $[Fe(CN)_6]^{3-}$ concentration in presence of these quenchers within 60 minutes. (e) EPR spectroscopy of DMPO solution to capture •OH radicals. (f) Detection of TEMPO by EPR spectroscopy. (g) The mechanism of CE-Chemistry in the flow tubes. (i) The process of electron transfer. (ii) CE oxidation by •OH radicals.

reactive radicals was estimated by terephthalic acid (THA) experiment. As illustrated in Fig. S8, the fluorescence emission intensity of the THA-•OH adduct (425 nm) increased after the THA solution flowed through the FEP tubes for 30 minutes, indicating the presence of •OH radicals during the FE process. The relationship between dissolved O_2 concentration and oxidation rate was further investigated by continuously bubbling air, N_2, or O_2, as illustrated in Fig. 3a. Prior to the reaction, the system was purged through the inlet for 15 minutes and then continuously bubbled throughout the reaction to ensure that the entire tubing was maintained under the target atmosphere. Fig. 3b demonstrates that the highest oxidation rate occurred during air bubbling, while the lowest rate was observed with O_2. This disparity arises primarily from the fact that oxidative environments impair the CE properties of the materials, leading to reduced electron induction and transfer during CE-Chemistry [22]. Furthermore, a series of radical and electron quenchers were added separately into the original solution, reaching 5 mM concentration of each quencher in solution, to investigate the CE-chemical performance. The evolution of $[Fe(CN)_6]^{3-}$ concentration in presence of these quenchers is displayed in Fig. 3c. 1–3 represents no additive, tertiary butanol (quencher for •OH radicals), and $AgNO_3$ (quencher for electrons), respectively. The results indicated that two kinds of intermediates, hydroxyl radicals (•OH) and electrons, might contribute to the oxidation of $[Fe(CN)_6]^{4-}$. Moreover, the electrons might be appeared as the limiting factor of FE process as less $[Fe(CN)_6]^{4-}$ was oxidized after 60 minutes when it was quenched (Fig. 3d). The UV absorption spectra of the two quenchers are illustrated in the Fig. S9. It is noticed that the absorption peak of tertiary butanol and $AgNO_3$ at 420 nm will not affect the absorption peak of $[Fe(CN)_6]^{3-}$ product. Electron paramagnetic resonance spectroscopy (EPR) was also carried out to directly confirm the production of radical intermediates. Specifically, 100 mM DMPO solution was utilized to capture •OH radicals, as illustrated by Fig. 3e. The curve inferred that quadruplet DMPO-•OH characteristic peaks were yielded when the fluid flows through FEP tubes, labeled by orange triangles, which can be ascribed to the fact that •OH radicals are more prone to react with DMPO and that the hydroxyl adduct is more stable than that of superoxide radicals. Fig. S10a exhibits the mechanism and characteristic peaks of DMPO capturing •OH radicals. Additionally, 2,2,6,6-Tetramethylpiperidine 1-oxyl (TEMPO), a paramagnetic electron quencher, were substantiated to capture electrons by EPR spectroscopy. Compared with the original peaks (labeled by blue stars), the peaks of TEMPO after CE-Chemistry, were decreased seen from EPR spectroscopy (Fig. 3**f**, from i to ii). It was because when TEMPO was reduced to TEMPOH due to capture of electrons, it lost its paramagnetic properties, resulting in a decreasing EPR signal (Fig. S10b). Electron transfer is paramount in solid-liquid CE and exerts a decisive influence on redox reactions, and the essence of CE-Chemistry possibly lies in the coupling of electron transfer with reactant interaction.

Therefore, the underlying mechanism of CE-Chemistry initiated by triboelectric charge of FE was depicted by Fig. 3g. During CE at the liquid-solid dielectric interface, electrons were firstly transferred from water to the FEP surface (step i) resulting in the negatively charged FEP surface and the generation of hydronium cations and •OH radicals. This process can be represented by the reaction (1) and (2). Moreover, •OH radicals in the diffusion layer (step ii) induced the CE-Oxidation reaction. On the other hand, the electron accumulated on the FEP tubes might adsorb hydronium cations in the vicinity of the solid surface forming the Stern layer. The EDL formation could inhibit the further interfacial electron transfer between DI water and FEP. However, as mentioned above, the reaction efficiency can be restored after cleaning the inner surface of FEP tubes with alcohol (Fig. 1d), demonstrating the recyclability and reusability of the FE method in CE-Chemistry.

2.4. Cascade reaction design and FIA simulation

Current methodologies for cascade reactions often rely on conventional setups such as continuous flow reactor, microreactor, multifunctional reactor, automated synthesis platform, batch reactor etc., which impose limitations on design flexibility and efficiency [23–26]. These limitations arise from the fact that approaches typically necessitate precise control of reaction conditions and often require complex configurations that can be challenging to optimize for specific applications. The greatest advantage of the dielectric tube reaction system induced by FE lies in its design flexibility and relatively minimized equipment cost. Beyond the physical design of the tubes to regulate chemical reactions, this system facilitates the implementation of diverse cascade reactions within dielectric tubes through electron transfer initiated by FE, thereby enhancing overall reaction efficiency. 2.0 mM luminol (dissolved in 30 mM NaOH, defined as benchmark luminol solution) and the mixed solution containing $K_4[Fe(CN)_6]$ and luminol flowed through the FEP tubes, respectively. It can be seen from Fig. 4a that the fluorescence intensity of luminol solution increased after CE-Chemistry reaction via FE for 120 minutes, presenting the effectiveness of the FE in the luminescence reaction. Moreover, the fluorescence emission intensity of the mixed solution is higher than that of the benchmark luminol solution, indicating the oxidation of $K_4[Fe(CN)_6]$ initiated via FE can enhance the luminol luminescence reaction, realizing the cascade reaction. In order to explore the role of $[Fe(CN)_6]^{4-}$ in the mixed solution, the UV absorption peaks of $[Fe(CN)_6]^{3-}$ in the mixed solution and pure $K_4[Fe(CN)_6]$ solution were tested every 30 minutes. The results were shown in the Fig. 4b. It can be observed that the UV-Vis absorbance intensity of oxidized $[Fe(CN)_6]^{3-}$ in the mixed solution is lower than that in the pure $K_4[Fe(CN)_6]$ solution. This phenomenon suggests that oxidized $[Fe(CN)_6]^{3-}$ reacts with luminol, thereby enhancing the luminescence of the cascade reaction. Consequently, the oxidation of $[Fe(CN)_6]^{4-}$ and the luminescence of luminol may occur simultaneously within the same reaction system. Fig. 4c illustrates that the fluorescence intensity of the mixed solution containing $K_4[Fe(CN)_6]$ and luminol increases over two hours, with a notable rise in the final hour, indicating that luminol may be oxidized by $[Fe(CN)_6]^{3-}$, resulting in fluorescence emission. The traditional mechanism of luminol chemiluminescence (CL) relies on highly reactive catalysts, such as hydrogen peroxide, $[Fe(CN)_6]^{3-}$, and horseradish peroxidase, which facilitate rapid oxidation to form 3-aminophthalate (3-APA*) in its excited state. Upon returning to its ground state, 3-APA* emits blue light at a wavelength of 425 nm [27,28]. Here, CE-Chemistry may contribute in two ways: directly oxidizing luminol and facilitating the oxidation of $[Fe(CN)_6]^{4-}$ to $[Fe(CN)_6]^{3-}$, which subsequently catalyzes the luminescence reaction of luminol (Fig. 4d). In flow injection analysis (FIA), the injection tubes enable the addition and separation of chemical reaction intermediates, inspiring the design of various cascade reactions.

Accordingly, the FIA reaction simulation is illustrated in Fig. 4**e**, where peristaltic pump I drives the FEP tubes to oxidize $[Fe(CN)_6]^{4-}$, while peristaltic pump II facilitates the oxidation of luminol to generate luminescence. Ultimately, the reaction solutions from the two peristaltic pumps are mixed. Compared with the benchmark luminol solution (1) and oxidized $[Fe(CN)_6]^{4-}$ via FE then mixed with the luminol solution (2), the fluorescence intensity of the mixed solution in Fig. 4e (3) was the highest (Fig. 4f). Figs. 4g and 4h illustrate the overview of FIA device and enlarged view of FIA sample detection system, respectively. A typical FIA device comprises several components: a sample injector, peristaltic pump, reaction coil, detector, and data processor (Fig. 4g). The FIA sample detection system encompasses these elements such as a sample auto-sampler, reagent reservoirs, injection port, reaction coil, flow tank and a control system for automated operation and data analysis (Fig. 4h). In analytical chemistry, FIA utilizes multiple injection tubes, enabling precise control over the addition or cessation of various liquids to create a mixed solution for analysis and detection. FIA is particularly well-suited for flow-based systems in CE-Chemistry, providing a framework for the design of more complex cascade reactions. It is important to note that the generation of FE is widely observed in flow-based systems. Previous studies on solid tubes and single droplets have demonstrated that FE can induce chemical

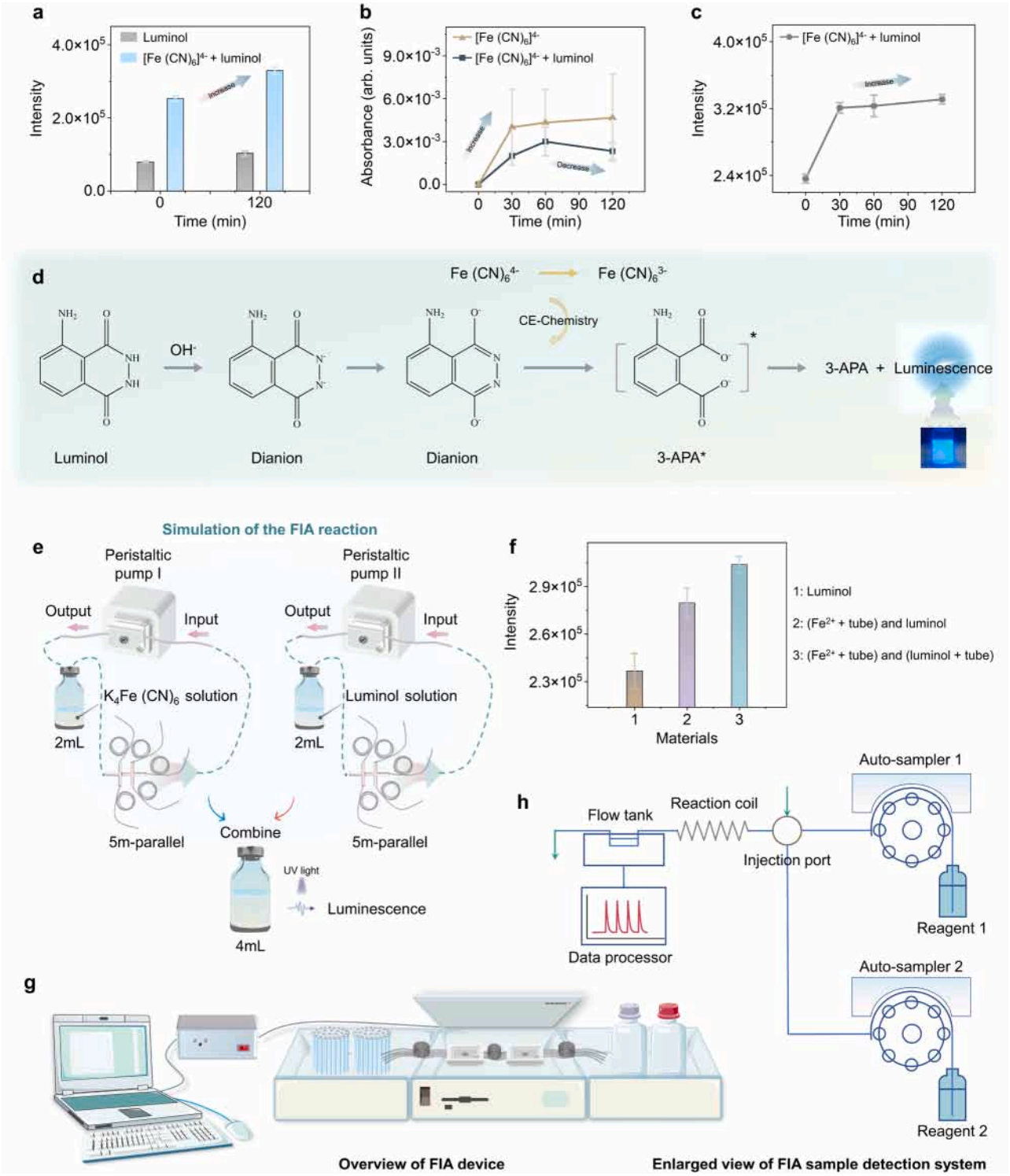

Fig. 4. Designing combinatorial reactions and simulation of the FIA. (a) The fluorescence emission intensity of luminol and mixed solution of ferrocyanide and luminol. (b) The UV absorption of $[Fe(CN)_6]^{3-}$ in potassium ferrocyanide solution and mixed solution. (c) The fluorescence emission intensity of the mixed solution at the corresponding time of b). (d) The mechanism of luminol luminescence during CE-Chemistry. (e) Simulation of the FIA reaction. (f) The fluorescence intensity of different solution. (g) Overview of FIA device. h) Enlarged view of FIA sample detection system.

reactions; however, the reaction efficiency resulting from FE in a single droplet is limited, hindering its ability to flexibly and effectively regulate chemical reactions [29]. Thus, it is anticipated that by emulating FIA, one can flexibly control and design desired chemical reactions using different inner walls of tubes with varied pathways as solid interfaces, facilitating flow between these walls and the continuous fluid to initiate reactions. In CE-Chemistry, conventional inert polymers such as FEP are widely employed as catalysts due to their CE properties. This capability enables the FEP tube to function as a long-distance solid flow channel that induces FE with the fluid, thereby serving both as a catalyst and as a reaction vessel with a flexible flow path design.

2.5. Contact-electro-chemistry induced by FE and its applications

Various chemical reactions can be initiated via CE-Chemistry induced by FE in dielectric tubes. To assess the feasibility of these reactions across different dielectric materials, PTFE tubes were employed to confirm the versatility of CE-Chemistry. The distinct CE properties of these dielectric tubes facilitate the investigation of the relationship between oxidation effects and their corresponding CE capabilities (Fig. S11). The variations in the oxidation level of $[Fe(CN)_6]^{4-}$ correspond to discrepancies in the CE performance of dielectric materials, with FEP exhibiting superior efficacy compared to PTFE. MO is typically found in wastewater from textile, dyeing, and paper industries, where it is used as a pH indicator and dye [30]. Its presence in effluents poses environmental concerns due to its toxicity and resistance to biodegradation [31,32]. Leveraging the enhanced CE performance of FEP tubes and an optimized reaction system design, we investigated the degradation of MO. As illustrated in Fig. 5a, a 0.01 mM MO solution was continuously flowed through the FEP tubes for 7 hours, with the initial surface charge refreshed using alcohol at hourly intervals. The results revealed a progressive degradation of MO over this duration, as indicated by the diminishing yellow color in Fig. 5b. Additionally, experiments utilizing the same FEP tubes over 4-hour intervals demonstrated consistent degradation performance after 7 cycles, as illustrated in Fig. 5c. Thus, this technique offers promising potential for wastewater treatment by facilitating the straightforward passage of wastewater through the tube. On the other hand, there are significant amounts of precious metals in electronic waste, catalytic converter waste and mining streams [33]. Recovering these metals is of great significance to sustainable development of the environment. Hence, in addition to degrading pollutants, the FE in the dielectric tubes was also investigated

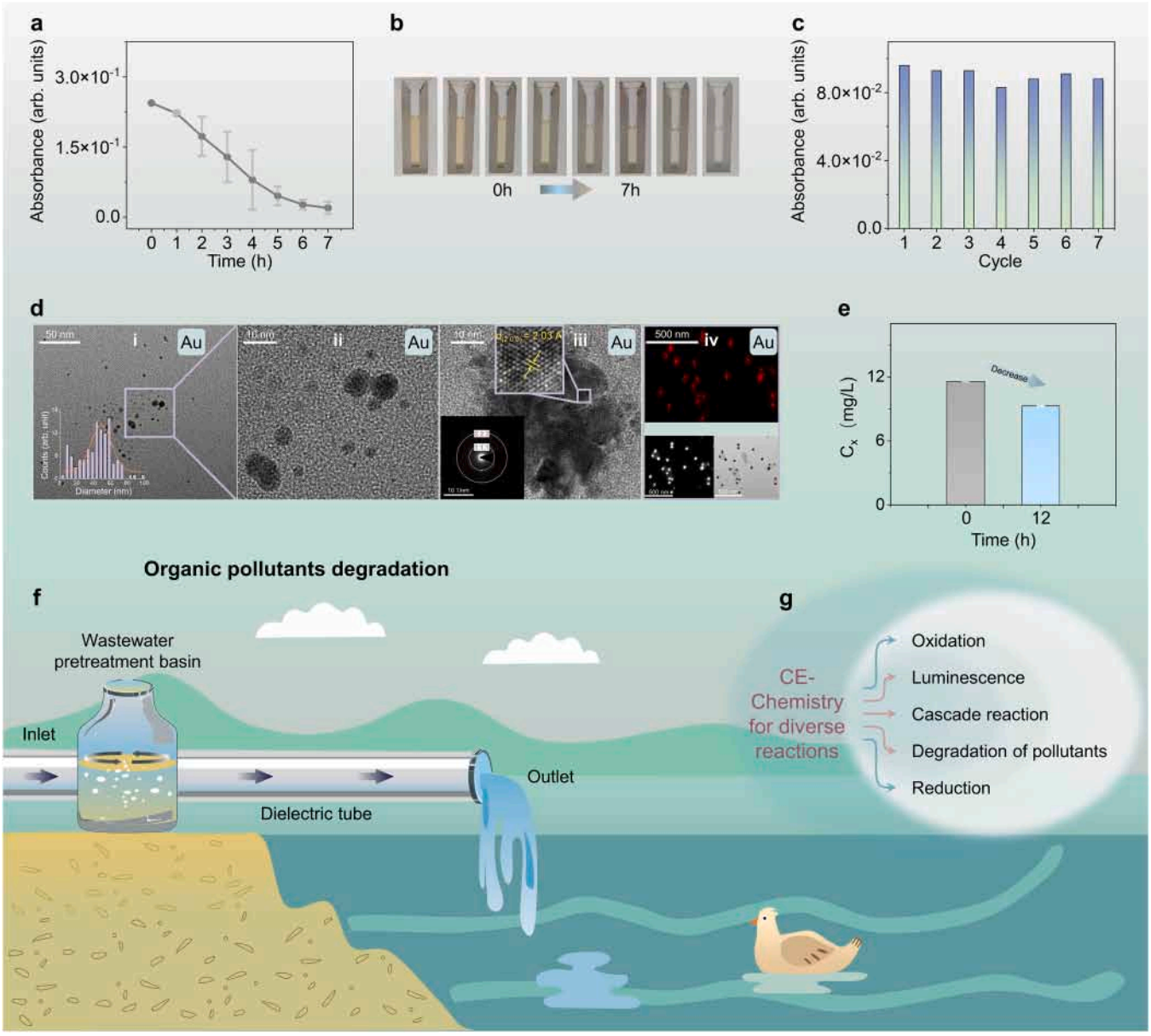

Fig. 5. Degradation of MO and reduction of $[AuCl_4]^-$ for pursuing potential applications in wastewater treatment. (a) MO solution flowing through the FEP tubes for 7 hours by removing the initial surface charge with alcohol every hour. (b) Optical photos of MO solution within 7 hours. (c) Recycling of FEP tubes for 7 cycles of 4 hours each time. (d) (i) TEM photograph and particle size distribution of Au^0 nanoparticles. (ii) Enlarged image of (i). (iii) Measurement of d-spacing on gold, the bottom left inset contains the SAED pattern of the particles. (iv) EDX mapping of gold, the bottom inset is HAADF and TEM images of the sample analyzed by EDX. (e) ICP-OES results of Au element after CE-Chemistry for12 hours. (f) Applicative prospect of organic pollutants and heavy metal solutions degradation. (g) Summary of the above reactions involved in CE-Chemistry.

to be used to drive the reduction of metal ions, such as the extraction of gold from 1 mM $KAuCl_4$ aqueous solution. Gold nanoparticles were extracted from the $KAuCl_4$ solution while flowing through the FEP tubes over a period of 12 hours, primarily via an electron transfer mechanism during the water-solid FE process. The solid precipitates obtained at the end of the gold reduction experiment were examined by high-resolution transmission electron microscope (HRTEM), as shown in Fig. 5d. The diameter of the obtained particles ranges from 40 nm to 60 nm (Fig. 5d (i)), with an enlarged view (Fig. 5d (ii)). It can be seen the particle adopts a spherical shape with aggregates. The Miller indices (h k l) and d-spacing (Fig. 5d (iii)) of one of the particles was obtained from Selected Area Electron Diffraction (SAED) and image analysis. A d-spacing of 2.03 Å on (2 0 0) plane was measured, which matched well with the data reported in the literature (PDF#99–0056). The particles contained gold element was confirmed through Energy Dispersive X-Ray (EDX) analysis, the corresponding high-angle annular dark-field (HAADF) and the transmission electron microscope (TEM) images in Fig. 5d (iv). Table S3 presented the results obtained for d-spacing of gold particle by analysis of the HRTEM and SAED. These results indicated that gold ions in solution have been effectively reduced to solid particles of Au^0, primarily due to electron transfer resulting from CE between the liquid and solid interfaces. Inductively Coupled Plasma Optical Emission Spectrometer (ICP-OES) results showed in Fig. 5e, indicating that the content of Au element decreased after 12 hours. The decrease may be caused primarily by the fact that the $[AuCl_4]^-$ ions in the original solution were extracted to form Au^0 nanoparticles after FE, and these particles had been centrifuged and filtered before ICP-OES test. These results supported the reduction of $[AuCl_4]^-$. Fig. 5f highlights the potential applications for the degradation of organic pollutants and heavy metal solutions. As wastewater traverses the long-distance dielectric tubes, it is anticipated to undergo gradual degradation, leading to enhanced energy efficiency and reduced emissions. Fig. 5g provides a comprehensive summary of the reactions involved in CE-Chemistry, encompassing oxidation/reduction, luminescence, cascade reactions, and the degradation of pollutants.

Moreover, FEP is a traditional inert polymer with stable physicochemical properties, offering the potential for large-scale use as both a reaction vessel and a CE catalyst. Importantly, as a CE catalyst, FEP does not participate in the chemical reaction itself. We conducted the following experiments to demonstrate this. The surface morphology, elemental composition, and group structures of FEP exhibited no significant changes before and after the CE-Chemistry, as evidenced by scanning electron microscope (SEM) images, EDX analysis (Fig. S12), X-ray photoelectron spectroscopy (XPS) (Fig. S13), Raman spectra, Fourier transform infrared (FTIR) spectra, and X-ray diffraction (XRD) patterns (Fig. S14). Specifically, morphological characterization and element mapping of FEP tubes before and after CE-Chemistry were reported in Figs. S12a and 12b. No morphological changes were observed, either by the naked eye or via SEM. Besides, the inserted EDS pictures indicated that the composition of FEP remained unchanged. Spectroscopic analysis techniques were also performed to deliver more in-depth information on the chemical properties of FEP tubes. XPS had been conducted to analyze the variation of the chemical state of FEP tubes before/after the CE-Chemistry. The C1s, F1s, and O1s spectra of the FEP tubes are listed in Figs. S13a-13c, respectively. Neither shift in binding energies of original peaks nor generation of new peaks was observed, which further confirmed the chemical stability of FEP. Fig. S14a presents the Raman spectroscopy, which the skeleton vibration pattern of FEP before and after the experiment is identical. FTIR spectroscopy results are shown in Fig. S14b. The fingerprint region in FTIR characterization, below 1500 cm^{-1}, was stable after the CE-Chemistry. XRD pattern of the dielectrics before and after CE-Chemistry showed no changes of chemical composition (Fig. S14c). These data indicated that the chemically inert FEP tubes act as catalysts for CE-Chemistry, suggesting that dielectrics can be reused with remarkable stability. This advantage facilitates environmentally friendly, non-metallic catalysis and enables complete recovery of the materials.

3. Conclusions

Flow electrification (FE), previously overlooked, is now recognized as a significant factor at solid-liquid interfaces, influencing chemical reactions within dielectric tubes. This study demonstrates that the physical design of these tubes, such as input flow velocity, inner diameter, length, and series-parallel configurations, can effectively modulate reaction rates, enabling tailored approaches to cascade reactions inspired by Flow Injection Analysis (FIA). The inert polymer FEP functions as both a reaction vessel and a CE catalyst, facilitating the degradation of organic pollutants and the recovery of precious metals while maintaining stability over multiple cycles. By leveraging the triboelectric charge from FE, this method allows for the monitoring of various chemical reactions, including the degradation of MO, the reduction of $[AuCl_4]^-$, the oxidation of $K_4[Fe(CN)_6]$, and the luminescence of luminol. Furthermore, the implications for analytical chemistry are profound, particularly in refining methodologies for flow systems such as HPLC, where undesired reactions may occur due to electrostatic charges generated by FE. This research highlights the potential of FE-induced reactions as a versatile and efficient tool in CE-Chemistry, offering significant advantages in stability, mildness, regulatory ease, and recyclability, ultimately advancing the interdisciplinary fields of broader interest in chemistry and physics.

4. Experimental

4.1. Reagents and materials

Potassium ferrocyanide [$K_4[Fe(CN)_6]$, HengXing, Analytical Reagent], potassium ferricyanide [$K_3[Fe(CN)_6]$, HengXing, Analytical Reagent], potassium chloride [KCl, HengXing, Analytical Reagent], tert-butanol [$C_4H_{10}O$, Sino-pharm Chemical Reagent Co., Ltd, 98 %], Silver nitrate ($AgNO_3$, Macklin, 99.8 %), 5,5-dimethyl-1-pyrroline N-oxide [DMPO, Dojindo], 2,2,6,6-tetramethylpiperidinooxy (TEMPO, $C_9H_{18}NO$, Macklin, 98 %), luminol [$C_8H_7N_3O_2$, Macklin 98 %], NaOH [Macklin 99.5 %], methyl orange (MO) [$C_{14}H_{14}N_3NaO_3S$, Macklin, 98 %], Potassium gold chloride ($KAuCl_4$, Macklin, Au≥51 %), fluorinated ethylene propylene (FEP) [Dupont], polytetrafluoroethylene (PTFE) [Dupont].

4.2. Sample preparation

A 2.0 mL sample solution containing 0.1 mM $K_4[Fe(CN)_6]$ was prepared in advance. Peristaltic pumps (BT100–2J) were used to promote the flow electrification (FE) of $K_4[Fe(CN)_6]$ solution in dielectric tubes. The temperature of this reaction was a constant temperature of 25 ℃. The solution of terephthalic acid was prepared by adding 332.4 mg of p-phthalic acid and 760 mg of sodium phosphate tribasic dodecahydrate. The mix solution of $K_4[Fe(CN)_6]$, tert-butanol and $AgNO_3$ were made by adding 1 mL 0.1 M pure tert-butanol and $AgNO_3$ solution to 19 mL 0.1 mM $K_4[Fe(CN)_6]$ solution, reaching 5 mM of the concentration of each additive, respectively. Samples for EPR analysis were prepared with 2.0 mL of DI water flowing in FEP tubes. The DMPO and TEMPO solution prepared for EPR analysis contained 2 μL DMPO and TEMPO per 2 mL of ultrapure water, respectively. A 2.0 mL luminol solution containing 2.0 mM luminol and 30.0 mM NaOH was prepared. The mixed solution of luminol and $[Fe(CN)_6]^{4-}$ contains 2.0 mM luminol and 0.1 mM $[Fe(CN)_6]^{4-}$. The dielectric tubes after reactions were cut along the wall of the tubes, then dried in an oven at 40 ℃ overnight before analysis. A 0.01 mM aqueous MO solution was prepared by adding 3.27 mg of $C_{14}H_{14}N_3NaO_3S$ in 1 L of ultrapure water. A 1 mM aqueous $KAuCl_4$ solution was prepared by adding 0.189 g of $KAuCl_4$ in 500 mL of ultrapure water.

4.3. Sample characterization

The UV-Vis absorptions of the samples were measured by UV-Vis spectrophotometer (UH4150) in a range of 200.0–600.0 nm. Fluorescence spectrometer (Edinburgh Instruments, full-featured, FLS980-S2S2-stm) was used to test luminol and THA-•OH luminescence intensity, using $\lambda_{excitation} = 375.0$ nm. Electron paramagnetic resonance (EPR) was recorded on a Bruker EMX plus-9.5/12/P/L. The measurements were conducted in X-Band (9.830243 GHz), with amplitude modulation of 1 G, microwave power of 2 mW, an amplitude modulation frequency of 100 kHz, conversion time of 60.00 ms, and a time constant at 40.96 ms. Morphologies of FEP tubes were observed by the scanning electron microscope (SEM SU8020, Hitachi). The Energy Dispersive X-Ray (EDX) analysis was conducted on FEI Nova 450 equipped with an AMETEK Octane Super appendix. The chemical states of dielectric materials before/after the CE-Chemistry were measured by near atmospheric pressure X-ray photoelectron spectrometer (NAP-XPS, SPECS, Germany). The Raman spectroscopy analysis was conducted on a LabRam HR evolution (HORIBA, SAS France), using a range from 300 to 1450 cm^{-1}. FTIR analysis was conducted on a Bruker Vertex 80 v on a range from 400 to 3000 cm^{-1}. X-ray diffraction (XRD) patterns of different solid dielectrics were acquired through an advance diffractometer (Bruker-D8, Germany) with a working voltage of 40 kV. HRTEM photographs and EDX mapping and spectra were obtained on a Tecnai G20 20 TWIN UEM. ICP-OES measurements were performed on an Agilent ICP-OES 730.

CRediT authorship contribution statement

Yuyang Zhang: Visualization, Software. **Ziming Wang:** Visualization, Software. **Zhong Lin Wang:** Writing – review & editing, Supervision, Funding acquisition, Conceptualization. **Di Wei:** Writing – review & editing, Supervision, Funding acquisition, Conceptualization. **Chong Xu:** Writing – original draft, Visualization, Validation, Methodology, Investigation. **Shaoxin Li:** Writing – review & editing, Investigation, Formal analysis.

Declaration of Competing Interest

The authors declare that they have no known competing financial interests or personal relationships that could have appeared to influence the work reported in this paper.

Acknowledgements

We would like to thank Ke Tian and Jiajin Liu for their assistance on data measurements. This work was supported by the National Natural Science Foundation (grant number 22479016).

Appendix A. Supporting information

Supplementary data associated with this article can be found in the online version at doi:10.1016/j.nanoen.2024.110526.

Data availability

Data will be made available on request.

References

[1] C. Moses, D. Robinson, J. Barlow, Methods for measuring rock surface weathering and erosion: a critical review, Earth Sci. Rev. 135 (2014) 141–161, https://doi.org/10.1016/j.earscirev.2014.04.006.
[2] A.F. White, S.L. Brantley, Chemical Weathering Rates of Silicate Minerals, De Gruyter, Berlin, Boston, 1995.
[3] M. Matsui, N. Murasaki, K. Fujibayashi, B. Peng You, Y. Kishimoto, Electrification of pure water flowing down a trough set up with a resin sheet, J. Electrost. 31 (1993) 1–10, https://doi.org/10.1016/0304-3886(93)90043-7.
[4] K. Yatsuzuka, Y. Mizuno, K. Asano, Electrification phenomena of pure water droplets dripping and sliding on a polymer surface, J. Electrost. 32 (1994) 157–171, https://doi.org/10.1016/0304-3886(94)90005-1.
[5] V.V. Yaminsky, M.B. Johnston, Static electrification by nonwetting liquids. contact charging and contact angles, Langmuir 11 (2002) 4153–4158, https://doi.org/10.1021/la00010a083.
[6] G. Gonella, E.H.G. Backus, Y. Nagata, D.J. Bonthuis, P. Loche, A. Schlaich, R. R. Netz, A. Kühnle, I.T. McCrum, M.T.M. Koper, M. Wolf, B. Winter, G. Meijer, R. K. Campen, M. Bonn, Water at charged interfaces, Nat. Rev. Chem. 5 (2021) 466–485, https://doi.org/10.1038/s41570-021-00293-2.
[7] Y. Wang, X. Wen, Y. Jia, M. Huang, F. Wang, X. Zhang, Y. Bai, G. Yuan, Y. Wang, Piezo-catalysis for nondestructive tooth whitening, Nat. Commun. 11 (2020) 1328, https://doi.org/10.1038/s41467-020-15015-3.
[8] Y. Wang, Y. Xu, S. Dong, P. Wang, W. Chen, Z. Lu, D. Ye, B. Pan, D. Wu, C. D. Vecitis, G. Gao, Ultrasonic activation of inert poly(tetrafluoroethylene) enables piezocatalytic generation of reactive oxygen species, Nat. Commun. 12 (2021) 3508, https://doi.org/10.1038/s41467-021-23921-3.
[9] J. Zhang, S. Lin, Z.L. Wang, Electrostatic charges regulate chemiluminescence by electron transfer at the liquid–solid interface, J. Phys. Chem. B 126 (2022) 2754–2760, https://doi.org/10.1021/acs.jpcb.1c09402.
[10] Y. Su, A. Berbille, Z.L. Wang, W. Tang, Water–solid contact electrification and catalysis adjusted by surface functional groups, Nano Res. 17 (2023) 3344–3351, https://doi.org/10.1007/s12274-023-6125-9.
[11] Z. Wang, X. Dong, W. Tang, Z.L. Wang, Contact-electro-catalysis (CEC), Chem. Soc. Rev. 53 (2024) 4349–4373, https://doi.org/10.1039/d3cs00736g.
[12] J. Zhao, X. Zhang, J. Xu, W. Tang, Z. Lin Wang, F. Ru Fan, Contact-electro-catalysis for direct synthesis of H_2O_2 under ambient conditions, Angew. Chem. Int. Ed. 62 (2023) e202300604, https://doi.org/10.1002/anie.202300604.
[13] A. Berbille, X.F. Li, Y. Su, S. Li, X. Zhao, L. Zhu, Z.L. Wang, Mechanism for generating H_2O_2 at water-solid interface by contact-electrification, Adv. Mater. 35 (2023) 2304387, https://doi.org/10.1002/adma.202304387.
[14] H. Li, A. Berbille, X. Zhao, Z. Wang, W. Tang, Z.L. Wang, A contact-electro-catalytic cathode recycling method for spent lithium-ion batteries, Nat. Energy 8 (2023) 1137–1144, https://doi.org/10.1038/s41560-023-01348-y.
[15] Y. Su, A. Berbille, X.-F. Li, J. Zhang, M. PourhosseiniAsl, H. Li, Z. Liu, S. Li, J. Liu, L. Zhu, Z.L. Wang, Reduction of precious metal ions in aqueous solutions by contact-electro-catalysis, Nat. Commun. 15 (2024) 4196, https://doi.org/10.1038/s41467-024-48407-w.
[16] S. Yao, X. Zhao, X. Wang, T. Huang, Y. Ding, J. Zhang, Z. Zhang, Z.L. Wang, L. Li, Bioinspired electron polarization of nanozymes with a human self-generated electric field for cancer catalytic therapy, Adv. Mater. 34 (2022) 2109568, https://doi.org/10.1002/adma.202109568.
[17] S. Li, J. Liu, Z.L. Wang, D. Wei, Mechano-driven chemical reactions, Green. Energy Environ. 24 (2024) https://doi.org/0.1016/j.gee.2024.08.001.
[18] S. Li, Z. Zhang, P. Peng, X. Li, Z.L. Wang, D. Wei, A green approach to induce and steer chemical reactions using inert solid dielectrics, Nano Energy 122 (2024) 109286, https://doi.org/10.1016/j.nanoen.2024.109286.
[19] J.R. Garratt, The internal boundary layer - a review, Bound. -Layer. Meteorol. 50 (1990) 171–203, https://doi.org/10.1007/bf00120524.
[20] D. Yoo, S. Jang, S. Cho, D. Choi, D.S. Kim, A liquid triboelectric series, Adv. Mater. 35 (2023) 2300699, https://doi.org/10.1002/adma.202300699.
[21] C. Xu, A.C. Wang, H. Zou, B. Zhang, C. Zhang, Y. Zi, L. Pan, P. Wang, P. Feng, Z. Lin, Z.L. Wang, Raising the working temperature of a triboelectric nanogenerator by quenching down electron thermionic emission in contact-electrification, Adv. Mater. 30 (2018) 1803968, https://doi.org/10.1002/adma.201803968.
[22] Z. Wang, A. Berbille, Y. Feng, S. Li, L. Zhu, W. Tang, Z.L. Wang, Contact-electro-catalysis for the degradation of organic pollutants using pristine dielectric powders, Nat. Commun. 13 (2022) 130, https://doi.org/10.1038/s41467-021-27789-1.
[23] A.A.H. Laporte, T.M. Masson, S.D.A. Zondag, T. Noël, Multiphasic continuous-flow reactors for handling gaseous reagents in organic synthesis: enhancing efficiency and safety in chemical processes, Angew. Chem. Int. Ed. 63 (2023) e202316108, https://doi.org/10.1002/anie.202316108.
[24] K.C. Nicolaou, D.J. Edmonds, P.G. Bulger, Cascade reactions in total synthesis, Angew. Chem. Int. Ed. 45 (2006) 7134–7186, https://doi.org/10.1002/anie.200601872.
[25] H.-M. Huang, M.H. Garduño-Castro, C. Morrill, D.J. Procter, Catalytic cascade reactions by radical relay, Chem. Soc. Rev. 48 (2019) 4626–4638, https://doi.org/10.1039/c8cs00947c.
[26] J. Jiao, W. Nie, T. Yu, F. Yang, Q. Zhang, F. Aihemaiti, T. Yang, X. Liu, J. Wang, P. Li, Multi-step continuous-flow organic synthesis: opportunities and challenges, Chem. – A Eur. J. 27 (2021) 4817–4838, https://doi.org/10.1002/chem.202004477.
[27] G. Merényi, J. Lind, T.E. Eriksen, Luminol chemiluminescence: chemistry, excitation, emitter, J. Biolumin. Chemilumin. 5 (2005) 53–56, https://doi.org/10.1002/bio.1170050111.
[28] J. Lind, G. Merenyi, T.E. Eriksen, Chemiluminescence mechanism of cyclic hydrazides such as luminol in aqueous solutions, J. Am. Chem. Soc. 105 (2002) 7655–7661, https://doi.org/10.1021/ja00364a032.
[29] Y. Zhao, Y. Liu, Y. Wang, S. Li, Y. Liu, Z.L. Wang, P. Jiang, The process of free radical generation in contact electrification at solid-liquid interface, Nano Energy 112 (2023) 108464, https://doi.org/10.1016/j.nanoen.2023.108464.

[30] Y. Kong, Z.-l Wang, Y. Wang, J. Yuan, Z.-d Chen, Degradation of methyl orange in artificial wastewater through electrochemical oxidation using exfoliated graphite electrode, N. Carbon Mater. 26 (2011) 459–464, https://doi.org/10.1016/s1872-5805(11)60092-9.
[31] A. Sahu, J.C. Poler, Removal and degradation of dyes from textile industry wastewater: benchmarking recent advancements, toxicity assessment and cost analysis of treatment processes, J. Environ. Chem. Eng. 12 (2024) 113754, https://doi.org/10.1016/j.jece.2024.113754.
[32] J. Sharma, S. Sharma, V. Soni, Classification and impact of synthetic textile dyes on aquatic flora: a review, Reg. Stud. Mar. Sci. 45 (2021) 101802, https://doi.org/10.1016/j.rsma.2021.101802.
[33] H. Lv, H. Huang, C. Huang, Q. Gao, Z. Yang, W. Zhang, Electric field driven delithiation: a strategy towards comprehensive and efficient recycling of electrode materials from spent lithium ion batteries, Appl. Catal. B: Environ. 283 (2021) 119634, https://doi.org/10.1016/j.apcatb.2020.119634.

Chong Xu received her B. S. degree in Material Chemistry from Civil Aviation University of China. Now she is a Ph.D. student at the University of Chinese Academy of Sciences (UCAS), and Beijing Institute of Nanoenergy and Nanosystems, Chinese Academy of Sciences. Her current research interest is contact-electro-chemistry.

Dr. Shaoxin Li is a post-doctor in the Beijing Institute of Nanoenergy and Nanosystems. She achieved the Ph.D. degree from the University of Chinese Academy of Sciences in 2022 and the B.S. degree from the Jiangsu University in 2017. Her research interest is self-powered sensors, energy harvesting, and solid-liquid contact electrification.

Yuyang Zhang received her B. S. degree in Jilin University, China. She is now studying in The Univerisity of Manchester, Department of Material Science. Her current research interest is multiscale simulation and machine learning.

Dr. **Ziming Wang** is currently a postdoctoral research fellow at the Beijing Institute of Nanoenergy and Nanosystems, Chinese Academy of Sciences. He received his Ph.D. degree in condensed matter physics from the University of Chinese Academy of Sciences (UCAS), under the supervision of Prof. Zhong Lin Wang. His research interests include contact-electro-catalysis, self-powered sensors, and energy harvesting.

Prof. **Zhong Lin Wang** received his Ph.D. from Arizona State University in physics. Dr. Wang has made original and innovative contributions to the synthesis, discovery, characterization and understanding of fundamental physical properties of oxide nanobelts and nanowires, as well as applications of nanowires in energy sciences, electronics, optoelectronics and biological science. His discovery and breakthroughs in developing nanogenerators established the principle and technological road map for harvesting mechanical energy from environment and biological systems for powering personal electronics. His research on self-powered nanosystems has inspired the worldwide effort in academia and industry for studying energy for micro-nano-systems, which is now a distinct disciplinary in energy research and future sensor networks. He coined and pioneered the field of piezotronics and piezophototronics by introducing piezoelectric potential gated charge transport process in fabricating new electronic and optoelectronic devices. Details can be found at: http://www.nanoscience.gatech.edu.

Prof. **Di Wei** serves as the Principal Investigator at BINN and heads the Iontronics Laboratory. As Fellow of the Royal Society of Chemistry (FRSC) and Senior Member of Wolfson College at Cambridge University, he has published over 100 papers including Nature Energy, Nature Commun., PNAS, Adv Mater, Energ Environ Sci., Matter etc. as the first/corresponding author. Prof. Wei also has a portfolio of over 200 international patents (including PCT). Notably, 57 international patents and 28 Chinese patents have been successfully granted, many of which have been transferred to leading companies like Nokia in Finland and Lyten in the USA. Additionally, Prof. Wei has edited three English books, published by Wiley and Cambridge University Press etc., focusing on nanotechnology for energy and sensor applications. Details can be found at: http://iontronics.group